RESEARCH ARTICLE

Mycological Characterization of *Coniochaeta luteoviridis* Isolated from an Ambrosia Beetle

Ju-Heon Lee[1,2], Youngsoo Kim[1], Jong-Taek Park[1], Dong-Hyuk Lee[1], Hye-Yeon Mun[3], Seung-Yoon Oh[4], and Hee-Young Jung[2*]

[1]Apple Research Center, National Institute of Horticultural & Herbal Science, Gunwi 43100, Korea
[2]Department of Plant Medicine, Kyungpook National University, Daegu 41566, Korea
[3]Fungal Research Team, Nakdonggang National Institute of Biological Resources, Sangju 37242, Korea
[4]Department of AI-Integrated Biological Sciences, Changwon National University, 20 Changwondaehak-ro, Changwon 51140, Korea

[*]Corresponding author: heeyoung@knu.ac.kr

ABSTRACT

In this study, fungal strain ARI-25-A13 was isolated from an ambrosia beetle collected using beetle traps deployed in an apple orchard. To achieve species-level identification, cultural and morphological characteristics, as well as molecular phylogenetic analyses, were conducted. On potato dextrose agar (PDA), colonies were initially salmon-colored and gradually transitioned to olive to brown with age, whereas colonies on malt extract agar (MEA) retained a salmon coloration throughout incubation. Morphologically, adelophialides were short, thin-walled, and inconspicuous, and neither collarettes nor discrete phialides were observed. Conidia were hyaline, ellipsoidal to cylindrical, frequently slightly curved, and measured 3.7–5.9 × 1.4–2.6 µm. Chlamydospores were hyaline, globose to ellipsoidal, formed terminally or intercalarily, occurring singly or in short chains, and measured 4.0–8.0 × 3.3–4.5 µm. Phylogenetic analysis based on the internal transcribed spacer (ITS), large subunit ribosomal DNA (LSU), β-tubulin (TUB), and actin (ACT) gene sequences placed ARI-25-A13 in the same clade as *Coniochaeta luteoviridis*. Collectively, the morphological traits and multilocus phylogenetic evidence support the identification of ARI-25-A13 as *C. luteoviridis*. This study provides the first mycological characterization of *C. luteoviridis* isolated from an ambrosia beetle.

Keywords: Ambrosia beetles, *Coniochaeta luteoviridis*, Morphology, Phylogeny

OPEN ACCESS

pISSN : 0253-651X
eISSN : 2383-5249

Kor. J. Mycol. 2026 June, 54(2):207–218
https://doi.org/10.4489/kjm.2026.54.2.10

Received: June 09, 2026
Revised: June 26, 2026
Accepted: June 30, 2026

INTRODUCTION

The genus *Coniochaeta* comprises a pleomorphic group of fungi within the family Coniochaetaceae [1], with *Coniochaeta ligniaria* designated as the type species. Currently, more than 100 species are recognized within the genus [2,3]. In earlier taxonomic frameworks, *Coniochaeta* was regarded as the sexual morph, whereas *Lecythophora* represented the corresponding asexual morph and was treated as a separate genus. Following the abolition of the dual nomenclature system for pleomorphic fungi, the older name *Coniochaeta* was conserved under the principle of nomenclatural priority, and species formerly assigned to

Lecythophora were transferred to *Coniochaeta* [4].

Morphologically, *Coniochaeta* species form white to salmon-colored or yellowish colonies, which may darken to olive or brown in the later stages of cultivation. Their conidia are produced phialidically and are ellipsoidal to cylindrical, and some species form globose to ellipsoidal chlamydospores [1].

Species of *Coniochaeta* have been documented across diverse ecological habitats, including wood, freshwater environments, and plant tissues, and have even been isolated from extreme environments such as uranium mines [3–5]. Numerous studies indicate that many members of the genus form endophytic associations with plants and typically remain asymptomatic. For instance, *Coniochaeta* spp. have been isolated from *Panax notoginseng* [6], *Coniochaeta endophytica* has been reported from healthy photosynthetic tissues of *Platycladus orientalis*, and *Coniochaeta ligniaria* has been isolated from leaves of *Baeckea frutescens*. Taken together, these findings indicate that *Coniochaeta* species predominantly exhibit an endophytic lifestyle [2,7].

Despite their frequent occurrence as endophytes, certain *Coniochaeta* species have been implicated in human infections. Notably, *C. hoffmannii* and *C. mutabilis* are recognized as opportunistic human pathogens and have been implicated in keratitis, subcutaneous abscesses, peritonitis, and endocarditis [8]. Moreover, several newly described *Coniochaeta* species originating from human and veterinary sources have been reported in recent years [9,10].

In Korea, the first case of fungemia caused by *C. hoffmannii* has been documented [11]. Beyond clinical occurrences, *C. ligniaria* has been isolated from leaves of *Abies koreana* [12], and *C. velutina* has been detected in indoor air samples, indicating a gradual expansion of domestic research on this genus.

In the present study, a *Coniochaeta*-like fungus was isolated from an ambrosia beetle known to cause damage to apple trees. To clarify its taxonomic placement, we conducted detailed morphological and molecular phylogenetic analyses, enabling species-level identification.

MATERIALS AND METHODS

Fungal isolation from ambrosia beetles

Ambrosia beetles were collected using traps installed in an orchard at the Apple Research Center, Gunwi-gun, Daegu-si, Republic of Korea (36°16′44.1″N, 128°27′56.2″E). Collected individuals were surface-sterilized by immersion in 70% ethanol for 1 min and subsequently air-dried at room temperature for approximately 10 min. Following surface sterilization, individual beetles were placed onto potato dextrose agar (PDA; Difco, Detroit, MI, USA) plates and incubated at 25°C. After 3 days of incubation, emerging fungal mycelia were transferred to fresh PDA plates and incubated for an additional 10 days at the same temperature to obtain pure cultures. The resulting single isolate was designated ARI-25-A13 and preserved in 20% glycerol at −80°C for long-term storage. In addition, the isolate was deposited in the Korean Agricultural Culture Collection (KACC) under accession number KACC 411349.

Morphological characterization

Isolate ARI-25-A13 was cultured on PDA and malt extract agar (MEA; Difco, Detroit, MI, USA) media at 25℃ for 14 days to assess its cultural and morphological characteristics. Colony diameter, pigmentation, and developmental changes were recorded throughout incubation. In addition, the morphological features of conidia and conidiophores were observed using a light microscope (CX-43, Olympus, Tokyo, Japan), and the dimensions of each structure were measured.

Genomic DNA extraction, PCR amplification, and sequencing

Genomic DNA was extracted from isolate ARI-25-A13 using the HiGene genomic DNA preparation kit (Biofact, Daejeon, Korea) following the manufacturer's protocol. Subsequently, the internal transcribed spacer (ITS) region and the large subunit of nuclear ribosomal RNA (LSU) region were sequenced to infer the genus-level identity of ARI-25-A13. For species-level identification, partial sequences of the translation elongation factor 1-alpha (TEF1-α), β-tubulin (TUB), and actin (ACT) genes were amplified by polymerase chain reaction (PCR).

The ITS region was amplified using primers ITS1F/ITS4 primer pair [13,14], and the LSU gene using LR0R/LR7 [15]. The TEF1-α gene was amplified with primers 983f/2218R [16], whereas TUB and ACT were amplified using BT1819R/BT2916 [17] and ACT-2/ACT-4r [18], respectively.

PCR products were separated on 1% agarose gels and visualized by ethidium bromide staining. Amplified fragments were purified using EXOSAP-IT reagent (Thermo Fisher Scientific, Waltham, MA, USA) in accordance with the manufacturer's protocol, and sequenced by Solgent Co., Ltd. (Daejeon, Korea).

Sequence assembly and analysis were carried out using SeqMan Lasergene software (DNAStar Inc., Madison, WI, USA). The ITS (LC928497), LSU (LC928498), TEF1-α (LC928499), TUB (LC928501), and ACT (LC928500) sequences obtained in this study were deposited in GenBank, with their accession numbers listed in Table 1.

Table 1. List of *Coniochaeta* species included in the phylogenetic analyses and their GenBank accession numbers

Species	Isolate	Isolation source	GenBank accession numbers			
			ITS	LSU	TUB	ACT
Coniochaeta acaciae	MFLUCC 17-2298T	Dead branches of Fabaceae	MG062735	MG062737	-	-
Coniochaeta arenariae	MFLUCC 18-0409	*Ammophila arenaria*	MN047126	MN017896	-	-
Coniochaeta africana	CBS 120868T	*Prunus salicina*	NR_137725	NG_066150	-	-
Coniochaeta baysunika	MFLUCC 17-0830T	*Rosa* sp.	MG828880	MG828996	-	-
Coniochaeta boothii	CBS 381.74T	Soil	NR_159776	AJ875226	-	-
Coniochaeta cateniformis	UTHSC 01-1644T	Canine bone marrow	NR_111517	HE610329	HE610347	HE610339
Coniochaeta canina	UTHSC 11-2460T	Canine breed German Shepard	NR_120211	NG_042720	-	-
Coniochaeta coluteae	MFLUCC 17-2299T	*Colutea paulsenii*	MG137251	MG137252	-	-
Coniochaeta decumbens	CBS 153.42T	Fruit	NR_144912	AF353597	-	-

Table 1. List of *Coniochaeta* species included in the phylogenetic analyses and their GenBank accession numbers(continued)

Species	Isolate	Isolation source	GenBank accession numbers			
			ITS	LSU	TUB	ACT
Coniochaeta deborreae	CBS 147215T	Soil	NR_173009	NG_076709	-	-
Coniochaeta discoidea	CBS 158.80T	Soil	NR_159779	NG_064120	-	-
Coniochaeta endophytica	AEA 9094T	*Platycladus orientalis*	EF420005	NG_075158	-	-
Coniochaeta euphorbiae	CBS 139768T	*Euphorbia polycaulis*	KP941076	KP941075	-	-
Coniochaeta fasciculata	CBS 205.38T	Butter	NR_154770	AF353598	HE610350	HE610342
Coniochaeta fibrosae	CGMCC3.20304T	*Candelaria fibrosa*	MW750760	MW750758	-	-
Coniochaeta fodinicola	CBS 136963T	Uranium mine	JQ904603	KF857172	-	-
Coniochaeta gigantospora	ILLS 60816T	Fraxinus Excelsior wood submerged In the river	NR_121521	JN684909	-	-
Coniochaeta hoffmannii	CBS 245.38T	Butter	NR_167688	MH867452	-	-
Coniochaeta iranica	CBS 139767T	*Euphorbia polycaulis*	KP941078	KP941077	-	-
Coniochaeta ligniaria	CBS 424.65T	*Picea abies*	MH858650	MH870292	-	-
Coniochaeta lignicola	CBS 267.33T	Unknown	NR_111520	NG_067344	HE610353	HE610345
Coniochaeta lignicola	CBS 590.63	Decaying wood	OQ429536	OQ055448		
Coniochaeta luteorubra	CBS 131710T	Leg wound	HE610330	HE610328	HE610346	HE610338
Coniochaeta luteoviridis	CBS 206.38T	*Picea abies*	NR_154769	NG_067348	HE610351	HE610343
Coniochaeta luteoviridis	IFM 50534	Unknown	AB190401	AB190429		
Coniochaeta luteoviridis*	**ARI-25-A13**	**Ambrosia beetle**	**LC928497**	**LC928498**	**LC928501**	**LC928500**
Coniochaeta marina	MFLUCC 18-0408T	From the sea, Leif Tibell	MK458764	MK458765	-	-
Coniochaeta monsterae	URM 8284T	Leaf endophytic *Monstera dansonii*	MZ648895	MZ648891	-	-
Coniochaeta mongoliae	CGMCC3.20250T	Medulla of *Ramalina sinensis*	MW077645	MW077646	-	-
Coniochaeta mutabilis	CBS 157.44T	*Picea abies*	NR_111519	NG_042382	HE610349	HE610341
Coniochaeta navarrae	CBS 141016T	On bark of *Ulmus* sp.	NR_154808	KU762326	-	-
Coniochaeta ostrea	CBS 507.70T	Twig of *Larrea* sp.	NR_159772	NG_064080	-	-
Coniochaeta polymorpha	CBS 132722T	Endotracheal aspirate of preterm Neonate	NR_121473	HE863327	HE863708	HE863709
Coniochaeta polysperma	CBS 669.77T	Dung of hare	MH861109	MH872868	-	-
Coniochaeta prunicola	CBS 120875T	*Prunus armeniaca*	NR_137037	NG_066151	-	-
Coniochaeta prunicola	HMJAU 34702	Rotten wood	MZ346578	MZ346514	-	-
Coniochaeta rosae	TASM 6127T	*Rosa hissarica*	NR_157509	NG_066204	-	-
Coniochaeta rosae	MFLUCC 17-0806	Branches	MG828882	MG828998		
Coniochaeta rhopalochaeta	CBS 109872T	*Bulnesia retamas*	NR_172554	GQ351561	-	-
Coniochaeta savoryi	CBS 725.74T	Wood of *Juniperus scopulorum*	MH860890	MH872627	-	-
Coniochaeta simbalensis	NFCCI 4236T	Soil	NR_164024	NG_068555	-	-
Coniochaeta sinensis	CGMCC3.20306T	Medulla of *Ramalina sinensis*	MW422269	MW422265	-	-
Coniochaeta velutina	CBS 981.68	bark beetle galleries of *Hylurgops palliatus*	MH859264	MH870991	-	-
Coniochaeta velutina	HMJAU 34693	Rotten wood	MZ346570	MZ346506	-	-
Coniochaeta vineae	KUMCC 17-0322T	On dead vine	NR_168225	MN473512	-	-
Coniochaeta verticillata	CBS 816.71T	Soil	NR_159774	AJ875232	-	-
Phialemonium obovatum	CBS 279.76T	Man, systemic mycotic infection in a six-month-old burned child	NR_165935	NG_057631	LT634002	HE599315

ITS, internal transcribed spacer; LSU, large subunit ribosomal DNA; TUB, β-tubulin; ACT, actin.
T: ex-type.
*The strain isolated in this study is shown in bold.

Molecular phylogenetic analysis

Each taxonomic marker sequence was subjected to a Basic Local Alignment Search Tool (BLAST) search against the NCBI database to assess sequence similarity. Based on these results, closely related strains were selected, and their sequence homology with ARI-25-A13 was evaluated.

The BLAST-based homology results were used to infer the genus to which ARI-25-A13 belongs and to guide the selection of molecular markers for phylogenetic reconstruction. Sequence alignment and phylogenetic analyses were conducted in MEGA 7 [19]. The sequences of the selected molecular markers were aligned using Clustal W, and the aligned sequences of the ITS, LSU, TUB, and ACT genes were concatenated for multilocus phylogenetic analysis.

Phylogenetic analysis was performed using the maximum likelihood (ML) method [20] under the Kimura two-parameter model [21], with gap positions excluded from the analysis. The reliability of the inferred phylogenetic tree was assessed by bootstrap analysis with 1,000 replicates.

RESULTS

Morphological characteristics of strain ARI-25-A13

On PDA at 25°C, colonies of ARI-25-A13 reached 20.3–21.2 mm in diameter after 7 days and 36.7–37.4 mm after 14 days. Colonies initially appeared salmon-colored and gradually transitioned to olive to brown as incubation progressed (Fig. 1A). On MEA under identical conditions, colony diameters were 9.0–9.5 mm after 7 days and 16.3–17.3 mm after 14 days. Colonies retained a salmon coloration throughout the incubation period (Fig. 1B). Adelophialides were short, thin-walled, and inconspicuous. Collarettes were not observed, and discrete phialides were absent (Fig. 1C–E). Conidia were produced in small groups of 2–4 at the apex. Chlamydospores were hyaline, globose to ellipsoidal, and formed terminally or intercalarily, occurring singly or in short chains. They measured 4.0–8.0 × 3.3–4.5 μm (mean 5.8 × 4.0 μm, Q = 1.5, n = 10) (Fig. 1F–G). Conidia were hyaline, ellipsoidal to cylindrical, frequently slightly curved, and measured 3.7–5.9 × 1.4–2.6 μm (mean 4.7 × 1.9 μm, mean Q = 2.5, n = 100) (Fig. 1H). Yellow-pigmented hyphae were occasionally observed and appeared as aggregated hyphal masses (Fig. 1I).

Fig. 1. Cultural and morphological characteristics of *Coniochaeta luteoviridis* ARI-25-A13. A: Front and reverse views of the colony grown on potato dextrose agar (PDA) for 14 days at 25°C. B: Front and reverse views of the colony grown on malt extract agar (MEA) for 14 days at 25°C. C–E: Adelophialides. F–G: Chlamydospores. H: Conidia. I: Yellow-pigmented hyphal aggregates. Scale bars: C–I = 10 μm.

Phylogenetic analysis

To elucidate the molecular and phylogenetic relationships of ARI-25-A13, sequences of the ITS and LSU regions and of the TEF1-α, ACT, and TUB genes were analyzed. Each sequence was compared with reference strains deposited in the NCBI database using BLAST searches.

The ITS sequence (586 bp) showed 100.0% similarity to *Coniochaeta luteoviridis* KoRLI047395 (GenBank no. MN341269), followed by *C. rosae* 4.27A (OP584633; 99.7%), *C. weberae* JKI-GP-23-051 (PV272675; 99.7%), *C. luteoviridis* CBS 206.38^{T} (MH855948; 99.3%), and *C. fasciculata* GSVCC22R3-2 (OR400651; 98.6%). The LSU sequence (1,289 bp) showed 100% similarity to *Coniochaeta luteoviridis* CBS 206.38^{T} (NG_067348.1), followed by *C. velutina* UAMH 10912 (EU999180; 99.8%), *C. cephalothecoides* L821 (KY064030; 99.1%), *C. hoffmannii* CBS 245.38^{T} (MG491499; 99.0%), and *C. endophytica* AEA 9094^{T} (NG_075158; 99.0%).

The TEF1-α sequence (905 bp) showed 98.8% similarity to *Coniochaeta lignicola* CBS 590.63 (OQ470829), followed by *C. fasciculata* CBS 205.38^{T} (MK693152; 98.7%) and *C. velutina* HMJAU 34696 (MZ465111; 98.5%). The ACT sequence (647 bp) showed the highest similarity to *Coniochaeta luteoviridis* CBS 206.38^{T} (HE610343; 99.0%), followed by *C. velutina* HMJAU 34693 (MZ464934; 96.2%), *C. lignicola* CBS 267.33^{T} (HE610345; 95.3%), and *C. fasciculata* CBS 205.38^{T} (HE610342; 95.3%). The TUB sequence (1,159 bp) showed the highest similarity to *Coniochaeta fasciculata* CBS 205.38^{T} (HE610350; 96.5%), followed by *C. luteoviridis* CBS 206.38^{T} (HE610351; 96.2%) and *C. lignicola* CBS 267.33^{T} (HE610353; 94.7%).

To determine the phylogenetic placement of ARI-25-A13, an ML phylogeny was constructed using concatenated ITS and LSU sequences. ARI-25-A13 clustered most closely with *C. luteoviridis* CBS 206.38^{T} with 76% bootstrap support, whereas its separation from the closely related *C. lignicola* was not strongly resolved in the combined ITS and LSU phylogeny (Fig. 2). To further refine its taxonomic position,

a multilocus phylogenetic analysis was conducted using ITS, LSU, TUB, and ACT sequences. The resulting ML phylogeny showed that ARI-25-A13 placed in a close relationship with *C. luteoviridis* CBS 206.38^{T} and was clearly separated from other species, including *C. lignicola* (Fig. 3).

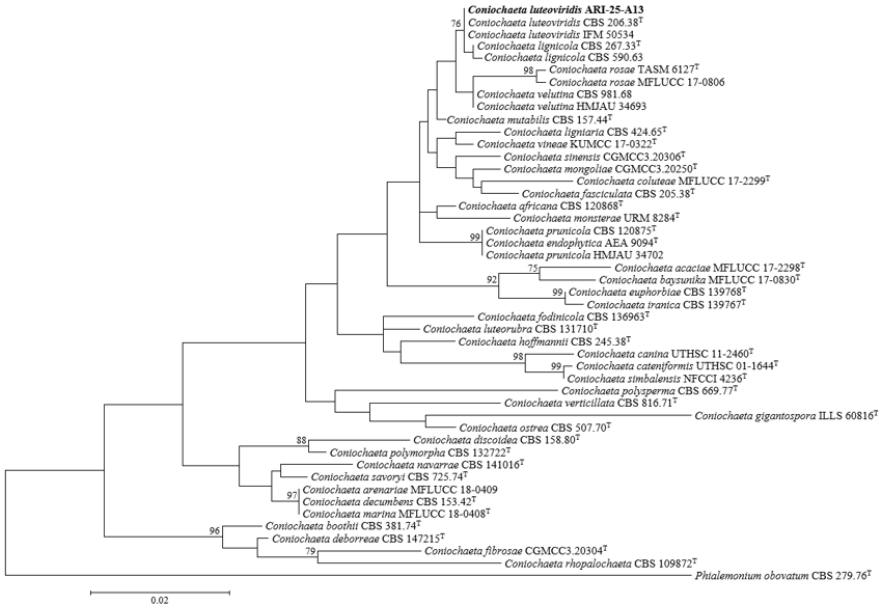

Fig. 2. Combined internal transcribed spacer (ITS) and large subunit ribosomal DNA (LSU) sequence data were used to infer a maximum-likelihood phylogenetic tree of *Coniochaeta*, in which the position of ARI-25-A13 is shown. Bootstrap values exceeding 70% from 1,000 replications are provided at the nodes. The isolate obtained in this study is indicated in bold. Phialemonium obovatum CBS 279.76^{T} was included as the outgroup. Scale bar = 0.02 substitutions per nucleotide position. 'T': ex-type.

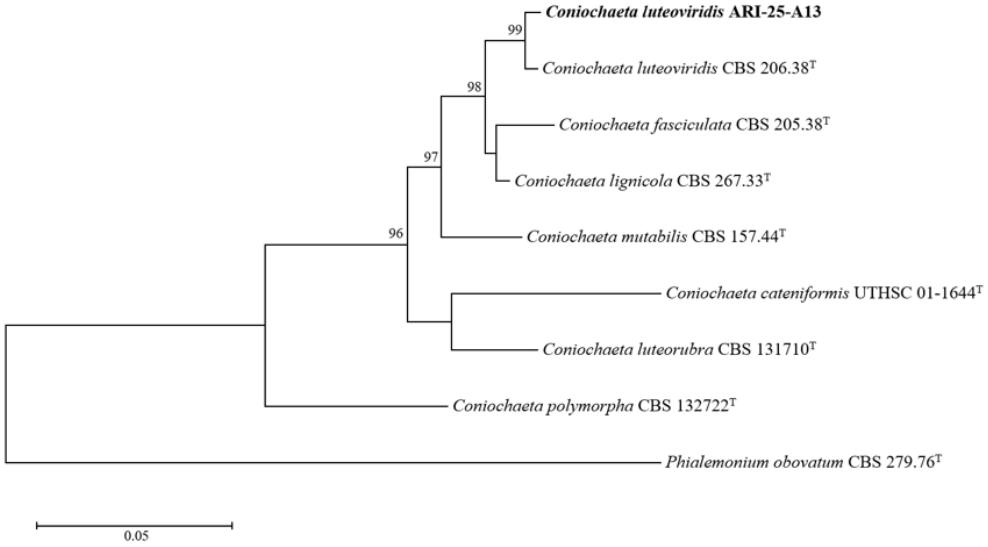

Fig. 3. Maximum-likelihood phylogenetic tree inferred from the combined internal transcribed spacer (ITS), large subunit ribosomal DNA (LSU), β-tubulin (TUB), and actin (ACT) sequences, showing the phylogenetic position of ARI-25-A13 among species of the genus *Coniochaeta*. Bootstrap values above 70% from 1,000 replications are presented at the nodes. The isolate obtained in this study is shown in bold. *Phialemonium obovatum* CBS 279.76^{T} was used as the outgroup. The scale bar indicates 0.05 substitutions per nucleotide position. 'T': ex-type.

Comparative analysis of cultural and morphological characteristics

Although ARI-25-A13 was phylogenetically related to both *Coniochaeta luteoviridis* and *C. lignicola*, its morphological characteristics more closely matched those of *C. luteoviridis*, whereas it was clearly distinguishable from *C. lignicola*.

On PDA, ARI-25-A13 exhibited an initial salmon coloration that gradually shifted to olive to brown with age, consistent with the documented color transition of *C. luteoviridis* CBS 206.38^{T} from salmon to olivaceous to brown on MEA (Table 2). In addition, ARI-25-A13 showed high similarity to *C. luteoviridis* CBS 206.38^{T} in conidial morphology, adelophialide characteristics, the absence of discrete phialides, and the presence and mode of formation of chlamydospores. Conidia of ARI-25-A13 (3.7–5.9 × 1.4–2.6 μm) were similar in shape to those of *C. luteoviridis* CBS 206.38^{T} (4.5–7 × 1.8–2.5 μm), although they were slightly smaller.

In contrast, *C. lignicola* has been reported to produce colonies that darken progressively with age, a pattern distinct from that of ARI-25-A13. Its conidia are described as ovoid to ellipsoidal, which distinguishes them from the somewhat curved conidia observed in ARI-25-A13. Conidia of *C. lignicola* CBS 267.33^{T} (3.0–4.5 × 1.5–2.0 μm) are also smaller and more uniform in shape than those of ARI-25-A13. Moreover, *C. lignicola* CBS 267.33^{T} is clearly distinguished from ARI-25-A13 by its conidiophore characteristics, particularly the predominance of discrete ventricose phialides and the presence of relatively long collarettes. The absence of chlamydospores in *C. lignicola* represents an additional diagnostic feature separating it from ARI-25-A13 (Table 2).

Table 2. Comparison of the morphological characteristics of isolate ARI-25-A13 with previously reported descriptions of *Coniochaeta luteoviridis* CBS 206.38^{T} and *C. lignicola* CBS 267.33^{T}

Characteristics		*C. luteoviridis* ARI-25-A13[a]	*C. luteoviridis* CBS 206.38^{T}[b]	*C. lignicola* CBS 267.33^{T}[b]
Colony	Color, Shape	Colony on PDA: initially salmon-colored, becoming olive to brown with age. Colony on MEA: remaining salmon-colored throughout the incubation period.	Colony on MEA: Initially salmon, later olivaceous to brown, surface covered with abundant aerial mycelium.	Colonies darkening with age.
	Size (mm)	Colonies on PDA attaining 36.7–37.4 mm diam after 14 days at 25°C; colonies on MEA attaining 16.3–17.3 mm diam after 14 days at 25°C.	Colonies on MEA attaining 29.0 mm diam after 14 days.	Colonies on MEA attaining 30.0–35.0 mm diam after 14 days.
Conidiophores	Color	Hyaline	N/A	N/A
	Shape	Adelophialides short, thin-walled, and inconspicuous, collarettes not observed, discrete phialides absent.	Adelophialides thin-walled and inconspicuous, with inconspicuous collarettes; discrete phialides not observed.	Adelophialides present but less abundant than discrete ventricose phialides, which are dominant and bear relatively long collarettes (1–1.5(–2) μm), cylindrical to slightly widened.
Conidia	Color	Hyaline	N/A	N/A
	Shape	Ellipsoidal to cylindrical, often slightly curved.	Ellipsoidal to cylindrical, sometimes slightly curved, containing small guttules.	Ovoidal to ellipsoidal, relatively small and regular in shape.
	Size (μm)	3.7–5.9 × 1.4–2.6	4.5–7.0 × 1.8–2.5	3.0–4.5 × 1.5–2.0
Chlamydospores	Color	Hyaline	Hyaline to faintly brown.	Not observed.
	Shape	Globose to ellipsoidal, formed terminally or intercalarily, occurring singly or in short chains.	Globose to ellipsoidal or pear-shaped, slightly thick-walled, terminal or intercalary, occurring singly or in short chains.	
	Size (μm)	4.0–8.0 × 3.3–4.5	4.0–13.0 × 3.5–6.0	

[T]ex-type strain; [a]Fungal strain studied in this paper; [b]Source of description [1].

DISCUSSION

In this study, ambrosia beetles were collected using traps deployed in an apple orchard, and strain ARI-25-A13 was isolated from these insects. Sequence analysis of the ITS rDNA region indicated that the isolate belonged to the genus *Coniochaeta*, and an integrated assessment of its morphological traits and multilocus phylogenetic relationships ultimately supported its identification as *Coniochaeta luteoviridis*.

Currently, approximately 170 species of *Coniochaeta* are registered in the MycoBank database. Despite the broad ecological distribution of this genus, species-level resolution based solely on ITS sequences remains challenging, as closely related taxa often cannot be reliably distinguished using this marker alone. Therefore, additional loci are required to achieve accurate species delimitation [2].

Recent studies on the classification and identification of novel *Coniochaeta* species have employed various molecular markers. Silva et al. [22] characterized *Coniochaeta monsterae* using ITS and LSU sequences, whereas Arnold et al. [23] used ITS and TEF1-α sequences to describe the new species *Coniochaeta elegans*, *C. montana*, and *C. nivea*, highlighting the utility of these loci for species-level identification within *Coniochaeta*. In addition, Kabtani et al. [3] employed ITS, LSU, TUB, and TEF1-α sequences for the classification and description of *C. massiliensis* as a novel species. Accordingly, in the present study, ITS, LSU, TUB, and TEF1-α, which have been frequently used in recent identification studies, were initially selected for the molecular characterization of ARI-25-A13.

Phylogenetic analyses based on the ITS and LSU genes revealed that ARI-25-A13 was most closely related to *C. luteoviridis*, although the phylogeny did not clearly resolve its separation from the closely related *C. lignicola*. To refine this placement, additional loci were considered; however, because the TEF1-α sequence of the type strain of *C. luteoviridis* was not available in the NCBI database, this marker could not be incorporated in the final phylogenetic analysis. As an alternative, the ACT and TUB genes, which were used by Perdomo et al. [9] for the description and identification of the novel species *C. luteorubra* and *C. cateniformis*, were selected and included in the multilocus phylogenetic analysis. However, ACT and TUB sequences are not available for many *Coniochaeta* species in the NCBI database, which limited the number of comparable strains. Nevertheless, all available strains possessing ACT and TUB sequence data were included in the analysis, allowing the phylogenetic position of ARI-25-A13 to be evaluated in relation to *C. luteoviridis* and *C. lignicola*. Ultimately, the multilocus phylogenetic analysis based on ITS, LSU, TUB, and ACT sequences showed that ARI-25-A13 consistently clustered with *C. luteoviridis* with strong statistical support.

Although ARI-25-A13 showed phylogenetic affinity to both *C. luteoviridis* and *C. lignicola*, its morphological characteristics were overall more congruent with those of *C. luteoviridis*. In particular, the pattern of colony color change on PDA, conidial morphology, adelophialide structure, the absence of discrete phialides, and the presence and mode of formation of chlamydospores all closely matched the diagnostic features of *C. luteoviridis*.

However, a difference between ARI-25-A13 and *C. luteoviridis* CBS 206.38^{T} was observed in growth rate on MEA. In the present study, ARI-25-A13 showed a colony diameter of 16.3–17.3 mm on MEA

after 14 days, whereas that of *C. luteoviridis* CBS 206.38^{T} was reported as 29.0 mm, indicating a notable difference in growth rate between the two strains. Although cultural characteristics have been considered in previous studies for distinguishing species of *Coniochaeta*, diagnostic traits such as colony color change, the morphology of conidiogenous cells, conidial morphology, and the presence or absence of chlamydospores have been regarded as more important than growth rate alone [4,22,24,25]. In addition, Weber [1] distinguished *C. luteoviridis* CBS 206.38^{T} from *C. velutina* mainly based on the presence of chlamydospores in *C. luteoviridis*, despite their overall morphological similarities. Therefore, the difference in growth rate on MEA observed in this study may have been influenced by differences in medium composition. Considering the overall agreement in morphological characteristics and multilocus phylogenetic results, ARI-25-A13 is best assigned to *C. luteoviridis*.

In Korea, a previous study investigated the distribution and diversity of endolichenic fungi from Jeju Island based on ITS sequence data and reported the occurrence of five *Coniochaeta* species, including *C. luteoviridis* [26]. However, species-level identification among closely related taxa may be limited when relying solely on the ITS region. In contrast, the present study clarified the phylogenetic position of ARI-25-A13 more precisely through multilocus phylogenetic analysis using ITS, LSU, TUB, and ACT sequences, and further presents the morphological characteristics of *C. luteoviridis*.

ARI-25-A13 was isolated from an ambrosia beetle. In general, ambrosia beetles are known to form symbiotic associations with fungi such as *Raffaelea* spp. and *Ambrosiella* spp. These insects typically colonize woody hosts, inoculate them with their symbiotic fungi, and subsequently utilize the fungal growth as a primary nutritional resource [27]. Species of *Coniochaeta* have also been isolated from wind-thrown stems of *Picea abies*, including *Coniochaeta ligniaria*, *C. velutina*, and *C. pulveracea*, and in particular, *C. malacotricha* has been reported from bark beetles and their galleries associated with *Picea* and *Pinus* [1]. However, current evidence is insufficient to determine whether species of *Coniochaeta* form a symbiotic relationship with ambrosia beetles or were merely isolated incidentally as endophytic fungi. Accordingly, it would be premature to exclude the possibility of an ecological association between these fungi and their insect hosts. Further studies and continued isolation and identification efforts will be necessary to clarify their ecological association.

CONFLICT OF INTEREST

The authors declare no conflict of interest.

ACKNOWLEDGMENTS

This work was supported by the "Cooperative Research Program for Agriculture Science and Technology Development (Project No. PJ017183)" funded by the Rural Development Administration, Republic of Korea. Additional support was provided by a grant from the Nakdonggang National Institute of Biological Resources (NNIBR), funded by the Ministry of Environment (MOE) of the Republic of Korea (NNIBR20261103).

REFERENCES

1. Weber E. The *Lecythophora-Coniochaeta* complex: I. Morphological studies on *Lecythophora* species isolated from *Picea abies*. Nova Hedwig 2002;74:159–85. https://doi.org/10.1127/0029-5035/2002/0074-0159
2. Harrington AH, del Olmo-Ruiz M, U'Ren JM, Garcia K, Pignatta D, Wespe N, Sandberg DC, Huang YL, Hoffman MT, Arnold AE. *Coniochaeta endophytica* sp. nov., a foliar endophyte associated with healthy photosynthetic tissue of *Platycladus orientalis* (Cupressaceae). Plant Fungal Syst 2019;64:65–79. https://doi.org/10.2478/pfs-2019-0008
3. Kabtani J, Militello M, Ranque S. *Coniochaeta massiliensis* sp. nov. isolated from a clinical sample28. J Fungi 2022;8:999. https://doi.org/10.3390/jof8100999
4. Khan Z, Gené J, Ahmad S, Cano J, Al-Sweih N, Joseph L, Chandy R, Guarro J. *Coniochaeta polymorpha*, a new species from endotracheal aspirate of a preterm neonate, and transfer of *Lecythophora* species to *Coniochaeta*. Antonie van Leeuwenhoek 2013;104:243–52. https://doi.org/10.1007/s10482-013-9943-z
5. Vázquez-Campos X, Kinsela AS, Waite TD, Collins RN, Neilan BA. *Fodinomyces uranophilus* gen. nov. sp. nov. and *Coniochaeta fodinicola* sp. nov., two uranium mine-inhabiting Ascomycota fungi from northern Australia. Mycologia 2014;106:1073–89. https://doi.org/10.3852/14-013
6. Wei G, Chen Z, Wang B, Wei F, Zhang G, Wang Y, Zhu G, Zhou Y, Zhao Q, He M, et al. Endophytes isolated from *Panax notoginseng* converted ginsenosides. Microb Biotechnol 2021;14:1730–46. https://doi.org/10.1111/1751-7915.13842
7. Kokaew J, Manoch L, Worapong J, Chamswarng C, Singburaudom N, Visarathanonth N, Piasai O, Strobel G. *Coniochaeta ligniaria* an endophytic fungus from *Baeckea frutescens* and its antagonistic effects against plant pathogenic fungi. Thai J Agric Sci 2011;44:123–31.
8. de Hoog GS, Guarro J, Gené J, Figueras MJ. Atlas of clinical fungi. 2nd ed. Utrecht: Centraalbureau voor Schimmelcultures; 2000.
9. Perdomo H, García D, Gené J, Cano J, Sutton DA, Summerbell R, Guarro J. *Phialemoniopsis*, a new genus of Sordariomycetes, and new species of *Phialemonium* and *Lecythophora*. Mycologia 2013;105:398–421. https://doi.org/10.3852/12-137
10. Troy GC, Panciera DL, Pickett JP, Sutton DA, Gene J, Cano JF, Guarro J, Thompson EH, Wickes BL. Mixed infection caused by *Lecythophora canina* sp. nov. and *Plectosphaerella cucumerina* in a German shepherd dog. Med Mycol 2013;51:455–60. https://doi.org/10.3109/13693786.2012.754998
11. Hong Y, Kim D, Park K, Sung H, Kim MN. The first case of *Coniochaeta hoffmannii* fungemia and literature review. Lab Med Online 2022;12:195–200. https://doi.org/10.47429/lmo.2022.12.3.195
12. Park H, Kim DY, Eom AH. Two unreported species of endophytic fungi isolated from leaves of *Abies koreana* in Korea. Kor J Mycol 2018;46:22–7. https://doi.org/10.4489/KJM.20180003
13. Gardes M, Bruns TD. ITS primers with enhanced specificity for basidiomycetes-application to the identification of mycorrhizae and rusts. Mol Ecol 1993;2:113–8. https://doi.org/10.1111/j.1365-294x.1993.tb00005.x
14. White TJ, Bruns TD, Lee SB, Taylor JW. Amplification and direct sequencing of fungal ribosomal RNA genes for phylogenetics. In: Innis MA, Gelfand DH, Sninsky JJ, White TJ, editors. PCR protocols: A guide to methods and applications. San Diego: Academic Press; 1990. p. 315–22. https://doi.org/10.1016/B978-0-12-372180-8.50042-1

15. Vilgalys R, Hester M. Rapid genetic identification and mapping of enzymatically amplified ribosomal DNA from several *Cryptococcus* species. J Bacteriol 1990;172:4238–46. https://doi.org/10.1128/jb.172.8.4238-4246.1990
16. Rehner SA, Buckley E. A *Beauveria* phylogeny inferred from nuclear ITS and EF1-α sequences: Evidence for cryptic diversification and links to *Cordyceps* teleomorphs. Mycologia 2005;97:84–98. https://doi.org/10.1080/15572536.2006.11832842
17. Miller AN, Huhndorf SM. Multi-gene phylogenies indicate ascomal wall morphology is a better predictor of phylogenetic relationships than ascospore morphology in the Sordariales (Ascomycota, Fungi). Mol Phylogenet Evol 2005;35:60–75. https://doi.org/10.1016/j.ympev.2005.01.007
18. Voigt K, Wöstemeyer J. Reliable amplification of actin genes facilitates deep-level phylogeny. Microbiol Res 2000;155:179–95. https://doi.org/10.1016/s0944-5013(00)80031-2
19. Kumar S, Stecher G, Tamura K. MEGA7: Molecular evolutionary genetics analysis version 7.0 for bigger datasets. Mol Biol Evol 2016;33:1870–4. https://doi.org/10.1093/molbev/msw054
20. Felsenstein J. Evolutionary trees from DNA sequences: A maximum likelihood approach. J Mol Evol 1981;17:368–76. https://doi.org/10.1007/bf01734359
21. Kimura M. A simple method for estimating evolutionary rates of base substitutions through comparative studies of nucleotide sequences. J Mol Evol 1980;16:111–20. https://doi.org/10.1007/bf01731581
22. Silva RM, Gonçalves CM, Oliveira TG, Oliveira RJ, Silva JM, Oliveira ML, Alves MV, Silva GA. *Coniochaeta monsterae*, sp. nov., (Coniochaetaceae, Coniochaetales): A new endophytic fungal species from Brazil. Sydowia 2023;75:283–92.
23. Arnold AE, Harrington AH, Huang YL, U'Ren JM, Massimo NC, Knight-Connoni V, Inderbitzin P. *Coniochaeta elegans* sp. nov., *Coniochaeta montana* sp. nov. and *Coniochaeta nivea* sp. nov., three new species of endophytes with distinctive morphology and functional traits. Int J Syst Evol Microbiol 2021;71:005003. https://doi.org/10.1099/ijsem.0.005003
24. Damm U, Fourie PH, Crous PW. *Coniochaeta* (*Lecythophora*), *Collophora* gen. nov. and *Phaeomoniella* species associated with wood necroses of *Prunus* trees. Persoonia 2010;24:60–80. https://doi.org/10.3767/003158510x500705
25. Crous PW, Carnegie AJ, Wingfield MJ, Sharma R, Mughini G, Noordeloos ME, Santini A, Shouche YS, Bezerra JDP, Dima B, et al. Fungal Planet description sheets: 868–950. Persoonia 2019;42:291–473. https://doi.org/10.3767/persoonia.2019.42.11
26. Oh SY, Yang JH, Woo JJ, Oh SO, Hur JS. Diversity and distribution patterns of endolichenic fungi in Jeju Island, South Korea. Sustainability 2020;12:3769. https://doi.org/10.3390/su12093769
27. Lee JH, Kim Y, Park JT, Lee DH, Jung HY. Morphological and phylogenetic characterization of *Raffaelea xyleboricola* sp. nov. from *Xyleborus* beetles in Korea. Mycobiology 2025;53:867–76. https://doi.org/10.1080/12298093.2025.2590303